

Three-Phase Grid-Connected Hybrid Generating System with Robust Nonlinear Controller

K.Swetha

M.Tech Student Scholar,

**Department of Electrical & Electronics Engineering,
KSRM College of Engineering,
Kadapa (Dt), A.P, India.**

P.Durga Prasad, M.Tech

Assistant Professor,

**Department of Electrical & Electronics Engineering,
KSRM College of Engineering,
Kadapa (Dt), A.P, India.**

ABSTRACT:

Micro grid systems consisting of several alternative energy sources that include solar cells, wind turbine, fuel cells and storage batteries are capable of balancing generated supply and demand resources to maintain stable service within a defined boundary. Wind and solar energy plays an important role in ensuring an environmental friendly and clean energy generation for remote and isolated areas. In this paper, a grid connected wind and PV hybrid generating system was developed with Robust Nonlinear Controller. The controller is designed based on the partial feedback linearization approach, and the robustness of the proposed control scheme is ensured by considering structured uncertainties within the PV system model. An approach for modeling the uncertainties through the satisfaction of matching conditions is provided. The superiority of the proposed robust controller is demonstrated on a test system through simulation results under different system contingencies along with changes in atmospheric conditions from the simulation results, it is evident that the robust controller provides excellent Performance under various operating conditions.

Keywords:

wind generator, Photovoltaic, Robust Nonlinear Controller, hybrid power generating system, power quality.

INTRODUCTION:

As generation and distribution companies in the market have been seeing an increasing interest in the renewable energy sources and also seeing demands from customers for higher quality and cleaner electricity, we are in need to switch over for renewable

energy generation methods. In order to reduce the greenhouse gas emission and to meet the demand of electricity, the trend converges to the use of renewable energy sources. Wind and PV energy technologies have a significant share in the use in hybrid power generating systems, because of emission free and no cost of energy. Hybrid wind and PV systems is one of the most efficient solution to supply power directly to a utility grid or to an isolated load [7]. Wind turbine converts kinetic energy of the wind into the mechanical energy and the mechanical energy is further converted into electrical energy by the wind Generator. Solar is a non – linear power source, whose radiation changes frequently, where the output power of the panel varies with temperature and isolation.

A single solar cell produce low voltage therefore several cells are combined to form modules to produce the desired voltage [1]. DC/AC inverter transfers the energy drawn from the wind turbine and PV into the grid as well as load by keeping common DC link constant. The inverter serves a dual role, to integrate hybrid systems to the grid and also to mitigate the harmonics and to improve the power quality problems due to nonlinear load. The proposed control strategy composes of an inner inductor current loop and a voltage loop in synchronous reference frame.

The inverter is regulated as the current source just by the inner inductor current loop in grid tied operation and the voltage controller is used to regulate the load voltage upon the occurrence of Islanding. The proposed control strategy is enhanced by introducing a unified load current feed forward, in order to deal with issues caused by non-linear local load and implemented by adding the load current is given to the

reference of inner current loop. In grid tied mode, DG injects harmonic current and therefore the harmonic component of the grid current will be mitigated [2], [3].

II. WIND AND SOLAR HYBRID SYSTEM:

A. Wind Power Generating System:

A hybrid energy system consists of two or more renewable energy sources to enhance system efficiency as well as greater balance in energy supply. Wind turbine is a device that converts kinetic energy of the wind into mechanical energy and the mechanical energy is again converted into electrical power. The power from the wind depends upon aerodynamically designed blades and rotor construction [6], [9]. The power in the wind is given by the kinetic energy of the flowing air mass per unit time and is expressed as

$$\begin{aligned} P_{air} &= \frac{1}{2} (\text{air mass per unit volume})^2 \\ &= \frac{1}{2} (\rho AV\infty) (V\infty)^2 \\ &= \frac{1}{2} \rho AV\infty^3 \end{aligned} \quad (1)$$

P_{air} - power contained in wind (in watts)

A - Swept area in (square meter)

$V\infty$ - wind velocity without rotor interference

Although Equation (1) gives the power available in the wind, the power transferred to the wind turbine rotor is reduced by the power coefficient, C_p

$$\begin{aligned} C_p &= P_{wind\ turbine} / P_{air} \\ P_{wind\ turbine} &= C_p * P_{air} \\ S &= \frac{1}{2} \rho AV\infty \end{aligned} \quad (2)$$

A maximum value of C_p is defined by the Betz limit, which states that a turbine can never extract more than 59.3% of the power from an air stream. In reality, wind turbine rotors have maximum C_p values in the range 25-45%. Variable speed wind turbine driving a Permanent Magnet Synchronous Generator (PMSG) is considered in this paper. PMSG is opted over other generators due to its advantages like, self-excitation property, which allows operation at high power factor and efficiency. PMSG also operates at low speed and thus the gearbox can be removed [4], [6].

B. PV Power Generating System:

The building block of PV arrays is the solar cell and it is basically a p-n junction diode that directly converts light energy into electricity. The cells are made of semiconductor materials, such as silicon, a thin semiconductor wafer is specially treated to form an electric field, positive on one side and negative on the other. A single PV cell generates 0.5V therefore several PV cells are connected in series and in parallel to form a PV module for desired output. The modules in PV array are usually first connected in series to obtain desired voltages; the individual modules are then connected in parallel to allow the system to produce more current [9], [11]. The PV mathematical model is represented by the following equation:

$$I = n_p I_{ph} - n_p I_{rs} [\exp^{q/KTA * V/ns} - 1]$$

I_{ph} - cell photo current

T - Cell temperature (k)

N_p - Number of cells in parallel

N_s - Number of cells in series

A - p-n junction ideality factor

III. STRUCTURE OF HYBRID POWER SYSTEM

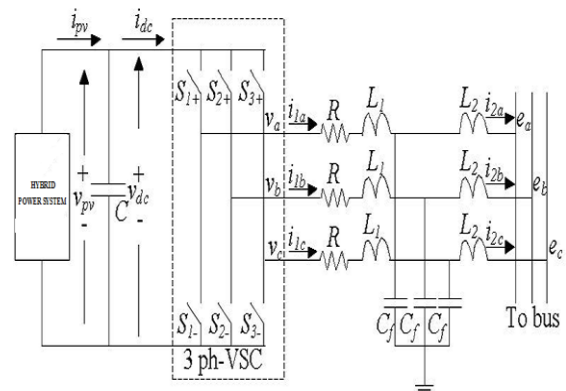


Fig.1 General Structure of the Proposed Model

A three-phase grid-connected PV with Wind is shown in Fig.1 where the PV with Wind array consists of a number of PV with Wind cells in a series and parallel combination to achieve the desired output voltage. The detailed modelling of a PV array and cell is given. The output voltage of the PV array is a dc voltage and, thus, the output dc power is stored in the dc-link capacitor.

The output current of the PV with Wind array is and that of the dc-link capacitor i_{scf} . The dc output power of the PV with Wind is converted into ac power through the inverter. The inverter, shown in Fig. 1, is a PV with Wind system with an output filter. insulated-gate bipolar transistor (IGBT)-based six-pulse bridge (S1+,S1-,S2+,S2-,S3+ , and S3-) in a three-phase voltage source converter (VSC) configuration since the PV with Wind system is connected to a three-phase grid supply point. The main purpose of this paper is to design a robust switching scheme for the IGBT-based six pulse bridge so that the PV with Wind system is capable of providing maximum power into the grid. The extraction of maximum power from the PV with Wind unit can be confirmed by monitoring the dc-link voltage (v_{pv}).

The output ac power of the inverter is supplied to the grid through the filters and connecting lines where the resistance of the connecting line R, L_1 and L_2 is and are the inductances of the filters and connecting lines and the filter capacitance is c_f . In Fig. 1, the grid voltages for phase A, phase B, and phase C are e_a, e_b and e_c respectively. The extracted maximum power from the PV with Wind system will be supplied to the grid if the output current of the inverter remains in phase with the grid voltage and, thus, it is essential to control this output current. In this section, a detailed model of a three-phase grid-connected PV with Wind system is developed based on the schematic shown in Fig.1 from Fig.1, it can be seen that there are two loops at the output side of the inverter. At first, by applying Kirchhoff's voltage law (KVL) at the inverter-side loop, the following equations can be obtained:

$$\begin{aligned} \dot{i}_{1a} &= -\frac{R}{L_1}i_{1a} - \frac{v_{cfa}}{L_1} + \frac{v_{pv}}{3L_1}(2K_a - K_b - K_c) \\ \dot{i}_{1b} &= -\frac{R}{L_1}i_{1b} - \frac{v_{cfb}}{L_1} + \frac{v_{pv}}{3L_1}(-K_a + 2K_b - K_c) \quad (3) \\ \dot{i}_{1c} &= -\frac{R}{L_1}i_{1c} - \frac{v_{cfc}}{L_1} + \frac{v_{pv}}{3L_1}(-K_a - K_b + 2K_c) \end{aligned}$$

where i_{1a}, i_{1b} and i_{1c} are the output currents of the inverter flowing through phase A, phase B , and phase

C , respectively; v_{cfa}, v_{cfb} and v_{cfc} are the voltages across the filter capacitor for phase A , phase B , and phase C, respectively; and K_a, K_b and K_c are the input switching signals for phase A , phase B , and phase C , respectively. By applying Kirchhoff's current law (KCL) at the dc-link capacitor node, the following equation can be obtained:

$$v_{pv} \dot{=} \frac{1}{C}(i_{pv} - i_{dc}) \quad (4)$$

The input current to the inverter can be written as [22]

$$i_{dc} = i_{1a}K_a + i_{1b}K_b + i_{1c}K_c \quad (5)$$

which yields

$$\dot{v}_{pv} = \frac{1}{C}i_{pv} - \frac{1}{C}(i_{1a}K_a + i_{1b}K_b + i_{1c}K_c) \quad (6)$$

If KCL is applied at the node where the filter capacitor C_f is connected, the following voltage – current relationships can be obtained

$$\begin{aligned} \dot{v}_{cfa} &= \frac{1}{C_f}(i_{1a} - i_{2a}) \\ \dot{v}_{cfb} &= \frac{1}{C_f}(i_{1b} - i_{2b}) \quad (7) \\ \dot{v}_{cfc} &= \frac{1}{C_f}(i_{1c} - i_{2c}) \end{aligned}$$

Where i_{2a}, i_{2b} and i_{2c} are the output currents of the LCL filter flowing through phase A, phase B, and phase C, respectively.

Finally by applying KVL at the grid-side loop, the state-space model can be written as

$$\begin{aligned} \dot{i}_{2a} &= \frac{1}{L_2}(v_{cfa} - e_a) \\ \dot{i}_{2b} &= \frac{1}{L_2}(v_{cfb} - e_b) \quad (8) \\ \dot{i}_{2c} &= \frac{1}{L_2}(v_{cfc} - e_c) \end{aligned}$$

The complete model of a three-phase grid-connected PV with Wind system is given by (3) and (6)–(8), which are nonlinear and time variant and this makes it difficult for implementing a simple control scheme [22].

The control problem is simplified by transforming the PV with Wind system model into a time-invariant model. This can be done by applying transformation using the angular frequency (ω) of the grid and considering the rotating reference frame synchronized with the grid where the component of the grid voltage is E_d , which means that is zero. By using transformation, (3) and (6) can be written in the form of the following group of equations:

$$\begin{aligned} \dot{I}_{1d} &= -\frac{R}{L_1} I_{1d} + \omega I_{1q} - \frac{v_{cf d}}{L_1} + \frac{v_{pv}}{L_1} K_d \\ \dot{I}_{1q} &= -\omega I_{1d} - \frac{R}{L_1} I_{1q} - \frac{v_{cf q}}{L_1} + \frac{v_{pv}}{L_1} K_q \\ \dot{v}_{pv} &= \frac{1}{C} i_{pv} - \frac{1}{C} I_{1d} K_d - \frac{1}{C} I_{1q} K_q \\ \dot{v}_{cf d} &= \omega v_{cf q} + \frac{1}{C_f} (I_{1d} - I_{2d}) \\ \dot{v}_{cf q} &= -\omega v_{cf d} + \frac{1}{C_f} (I_{1q} - I_{2q}) \\ \dot{I}_{2d} &= -\omega I_{2q} + \frac{1}{L_2} (v_{cf d} - E_d) \\ \dot{I}_{2q} &= -\omega I_{2d} + \frac{1}{L_2} (v_{cf q} - E_q) \end{aligned} \quad (9)$$

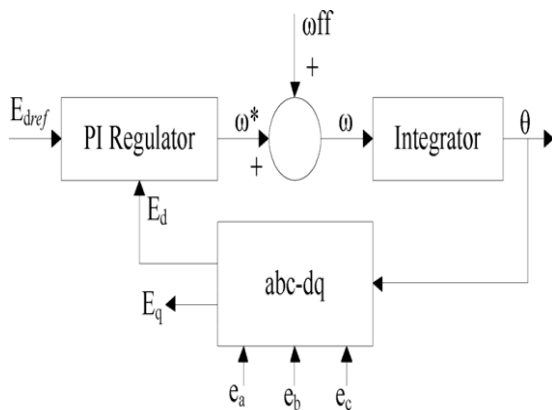


Fig. 2. PLL model.

where K_d and K_q are the switching signals in the dq frame, and, $I_{dq} = T_{abc}^{dq} i_{abc}$, $e_{dq} = T_{abc}^{dq} e_{abc}$, $K_{dq} = T_{abc}^{dq} K_{abc}$ and the transformation matrix T_{abc}^{dq} can be written as

$$T_{abc}^{dq} = \frac{2}{3} \begin{pmatrix} \cos \omega t & \cos(\omega t - 120) & \cos(\omega t + 120) \\ \sin \omega t & \sin(\omega t - 120) & \sin(\omega t + 120) \\ \frac{1}{2} & \frac{1}{2} & \frac{1}{2} \end{pmatrix} \quad (10)$$

The group of (9) represents the complete mathematical model of a three-phase grid-connected PV with Wind system with an output filter, and this model is a nonlinear model due to the nonlinear behavior of the switching signals and the output current (i_{pv}) of the PV with Wind. But in a practical system, it is essential to use a phase-locked loop (PLL) for instantaneous tracking of grid frequency. The dynamical of the PLL used in this paper is mainly based on the approach as presented in which is shown in Fig. 2 In this PLL model, E_{dref} represents the reference value of the direct-axis grid voltage, ω^* indicates the measured angular frequency, and ω_{ff} is the feed forward angular frequency.

As mentioned earlier in this section, the robust nonlinear control scheme needs to be designed in such a way that it is capable of controlling the dc-link voltage (v_{dc}) and the output current of the inverter. Since the d component of the grid voltage is zero, the d component current will not affect the maximum power delivery and it is essential to control the q component current. From the mathematical model as represented by (9), it can be seen that the dynamics of the component output current (I_{2q}) of the filter do not have the relationship with the switching signals. But the dynamics of the inverter output current (I_{1q}) have a coupling with the switching signal and, therefore, I_{1q} is chosen as another control objective. An overview of designing the partial feedback linearizing controller is discussed in the following section by considering v_{dc} and I_{1q} as control objectives.

III. OVERVIEW OF FEEDBACK LINEARIZING THE CONTROLLER DESIGN

Since the three-phase grid-connected PV with Wind system, as represented by the group of (9), has two control inputs (K_d and K_q) and the controller needs to be designed with two control objectives (V_{dc} and I_{1q}), the mathematical model can be represented by the following form of a nonlinear multi-input multi output (MIMO) system

$$\begin{aligned} \dot{x} &= f(x) + g_1(x)u_1 + g_2(x)u_2 \\ y_1(x) &= h_1(x) \end{aligned} \quad (11)$$

$$y_2(x) = h_2(x)$$

Where

$$x = [I_{1d} \quad I_{1q} \quad v_{pv} \quad v_{cfd} \quad v_{cfq} \quad I_{2d} \quad I_{2q}]^T$$

$$f(x) = \begin{bmatrix} -\frac{R}{L_1} I_{1d} + \omega I_{1q} - \frac{v_{cfd}}{L_1} \\ -\omega I_{1d} - \frac{R}{L_1} I_{1q} - \frac{v_{cfq}}{L_1} \\ \frac{1}{C} i_{pv} \\ \omega v_{cfq} + \frac{1}{C_f} (I_{1d} - I_{2d}) \\ -\omega v_{cfd} + \frac{1}{C_f} (I_{1q} - I_{2q}) \\ \omega I_{2q} + \frac{1}{L_2} (v_{cfd} - E_d) \\ -\omega I_{2d} + \frac{1}{L_2} (v_{cfq} - E_q) \end{bmatrix}$$

$$g(x) = \begin{bmatrix} \frac{v_{pv}}{L_1} & 0 \\ 0 & \frac{v_{pv}}{L_1} \\ -\frac{I_{1d}}{C} & -\frac{I_{1q}}{C} \\ 0 & 0 \\ 0 & 0 \\ 0 & 0 \\ 0 & 0 \end{bmatrix}$$

$$u = [K_d \quad K_q]^T$$

And

$$y = [I_{1q} \quad v_{pv}]^T$$

The design of a partial feedback linearizing controller depends on the feedback linearizability of the system, and this feedback linearizability is defined by the relative degree of the system. The relative degree of the system, in turn, depends on the output functions of the system. The nonlinear model of a three-phase grid-connected PV with Wind system as shown by (11) can be linearized using feedback linearization when some conditions are satisfied. Consider the following nonlinear coordinate transformation ($z = \phi(x)$) for the aforementioned three-phase grid-connected PV with Wind system:

$$z = [h_1 L_f h_1 \quad \dots L_f^{r_1-1} h_1 \quad h_2 L_f h_2 \quad \dots L_f^{r_2-1} h_2]^T \quad (12)$$

Where $r_1 < n$ and $r_2 < n$ are the relative degrees corresponding to output functions $h_1(x)$ and $h_2(x)$, respectively; $L_f h_i(x) = (\partial h_i) / (\partial x) f(x)$ are the Lie derivative $h_i(x)$, $i = 1, 2, \dots$ of $f(x)$. The change of coordinate (12) transforms the nonlinear system (11) from to coordinates provided that the following conditions are satisfied for:

$$L_g L_f^k h_i(x) = 0; k < r_i - 1$$

$$L_g L_f^{r_i-1} h_i(x) \neq 0 \quad (13)$$

$$n = \sum_{i=1}^n r_i$$

where $L_g L_f^k h_i(x)$ is the Lie derivative $L_f^k h_i(x)$ of along $g(x)$. The linearized system can be expressed as follows:

$$\dot{z} = A(x) + B(v) \quad (14)$$

Where A is the system matrix, B is the input matrix, and v is the new linear control input for the feedback linearized system. When $(r_1+r_2) < n$; only partial feedback linearization is possible, that is, some states are transformed through nonlinear coordinate transformation and some are not. The new states of a partially feedback linearized system can be written as

$$z = \phi(x) = [\tilde{z} \quad \hat{z}] \quad (15)$$

where \tilde{z} represents the state vector obtained from nonlinear coordinate transformation of order (r_1+r_2) and is the state vector of the nonlinear (remaining) part of order $n - (r_1+r_2)$. The dynamic of \tilde{z} is called the internal dynamics of the system which need to be stable in order to design and implement a partial feedback linearizing controller for the following partially linearized system:

$$\dot{\tilde{z}} = \tilde{A}\tilde{z} + \tilde{B}\tilde{v} \quad (16)$$

Where \tilde{A} is the system matrix, \tilde{B} is the input matrix, and \tilde{v} is the new linear control input for the partially linearized system, and any linear controller design technique can be employed to obtain the linear control law for the partially linearized system. But before obtaining a robust control law through the proposed approach, it is essential to model the uncertainties and to ensure the partial feedback linearizability of the PV system along the stability of internal dynamics which are not linearized through the transformation. The details of uncertainty modeling are discussed in the following section.

IV. UNCERTAINTY MODELING:

As mentioned earlier, the output power of the PV system depends on the intensity of the solar irradiation which is uncertain because of unpredictable changes in weather conditions. These changes may be modeled as uncertainties in current out of the solar panels (i_{pv}) which, in turn, causes uncertainties in the current (in the dq-frame, I_{1d} , I_{1q} , I_{2d} , and I_{2q}) injected into the grid. Since the uncertainty in the output power of inverters is related to the frequency of the grid, the proposed scheme has the capability of accounting for the uncertainty in the grid frequency. In addition, the parameters used in the PV model are, in most cases, either time varying or not exactly known and, therefore, parametric uncertainties exist too. Thus, it is essential to represent these uncertainties in PV system models. In the presence of uncertainties, a three-phase grid-connected PV system can be represented by the following equation:

$$\begin{aligned} \dot{x} &= [f(x) + \Delta f(x)] + [g_1(x) + \Delta g_1(x)]u_1 \\ &\quad + [g_2(x) + \Delta g_2(x)]u_2 \\ y_1 &= h_1(x) \\ y_2 &= h_2(x) \end{aligned} \quad (17)$$

Where

$$\Delta f(x) = \begin{bmatrix} \Delta f_1(x) \\ \Delta f_2(x) \\ \Delta f_3(x) \\ \Delta f_4(x) \\ \Delta f_5(x) \\ \Delta f_6(x) \\ \Delta f_7(x) \end{bmatrix}$$

And

$$\Delta g(x) = \begin{bmatrix} \Delta g_{11}(x) & 0 \\ 0 & \Delta g_{22}(x) \\ \Delta g_{31}(x) & \Delta g_{32}(x) \\ 0 & 0 \\ 0 & 0 \\ 0 & 0 \\ 0 & 0 \end{bmatrix}$$

Which are uncertainties in $f(x)$ and $g(x)$, respectively. To formulate the robust controller design problem, we assume that the structure of state –dependent

uncertainties and the nature of parametric uncertainties satisfy the following conditions.

$$\Delta f(x) \text{ and } \Delta g(x) \in \text{span} \{g(x)\} \quad (18)$$

If these matching conditions hold, then the following condition holds too:

$$\omega \geq r = \rho \quad (19)$$

Where r is the total relative degree of the nominal system (11) which for the system under study is 2, ω is the relative degree of uncertainty $\Delta g(x)$, ρ and is the relative degree of uncertainty $\Delta f(x)$. In order to match the uncertainties with the PV system model, the relative degree of the uncertainty Δf should be equal to the relative degree of the nominal system 2, This can be calculated from the following equations:

$$\begin{aligned} L_{\Delta f} L_f^{1-1} h_1(x) &= \Delta f_2 \\ L_{\Delta f} L_f^{1-1} h_2(x) &= \Delta f_3 \end{aligned} \quad (20)$$

If the relative degree of Δf is 1 for each output h_1 and h_2 , then the total relative degree of Δf will be 2. This will be the case if Δf_2 and Δf_3 are not equal to zero. To match the uncertainties in Δg , the relative degree of Δg should be equal to or greater than the total relative degree of the nominal system. It will be 2 if the following conditions hold:

$$\begin{aligned} L_{\Delta g} L_f^{1-1} h_1(x) &= \Delta g_{11}(x) \neq 0 \\ L_{\Delta g} L_f^{1-1} h_2(x) &= \Delta g_{31} + \Delta g_{32} \neq 0 \end{aligned} \quad (21)$$

Since the proposed uncertainty modeling scheme considers the upper bound on the uncertainties, these bounds should be set to proceed with the robust controller design. If the maximum-allowable changes in the system parameters are set to 30% and the variations in solar irradiation and environmental temperature are set to 80% of their nominal values, then the upper bound on uncertainties Δf and Δg for the PV system under study can be obtained as

$$\Delta f(x) = \begin{bmatrix} -0.025 \frac{R}{L_1} I_{1d} + 0.6\omega I_{1q} - 0.23 \frac{V_{cfd}}{L_1} \\ -0.36\omega I_{1d} - 0.042 \frac{R}{L_1} I_q - 0.23 \frac{V_{cfq}}{L_1} \\ 0.16 \frac{1}{C} i_{pv} \\ 0.2\omega v_{cfq} + 0.72 \frac{1}{C_f} (I_{1d} - I_{2d}) \\ -0.12\omega v_{cfd} + 1.2 \frac{1}{C_f} (I_{1q} - I_{2q}) \\ 0.6\omega I_{2q} + \frac{2}{L_2} (0.12v_{cfd} - E_d) \\ -0.36\omega I_{2d} + \frac{2}{L_2} (0.2v_{cfd} - E_q) \end{bmatrix} \quad (22)$$

And

$$\Delta g(x) = \begin{bmatrix} 0.18 \frac{V_{pv}}{L_1} & 0 \\ 0 & 0.18 \frac{V_{pv}}{L_1} \\ -0.08 \frac{I_{1d}}{C} & -0.14 \frac{I_{1q}}{C} \\ 0 & 0 \\ 0 & 0 \\ 0 & 0 \\ 0 & 0 \end{bmatrix} \quad (23)$$

The partial feedback linearizing scheme, cannot stabilize the PV system appropriately if the aforementioned uncertainties are considered within the PV system model since the controller is designed to stabilize only the nominal system. However, in the robust partial feedback linearizing scheme, the aforementioned uncertainties need to be included to achieve the robust stabilization of the grid-connected PV system. The robust controller design by considering the aforementioned uncertainties within the grid-connected PV system model is shown in the following section.

V. ROBUST CONTROLLER DESIGN:

The following steps are followed to design the robust controller for a three-phase grid-connected PV system as shown in Fig. 1.

Step 1: Partial feedback linearization of grid-connected PV systems.

In this case, the partial feedback linearization for the system with uncertainties can be obtained as

$$\begin{aligned} \dot{\hat{z}}_1 &= L_f h_1(x) + L_{\Delta f} h_1(x) + [L_{g_1} h_1(x) + h_1(x)] u_1 \\ &\quad + [L_{g_2} h_1(x) + L_{\Delta g_2} h_1(x)] u_2 \\ \dot{\hat{z}}_2 &= L_f h_2(x) + L_{\Delta f} h_2(x) + [L_{g_1} h_2(x) + L_{\Delta g_2} h_2(x)] u_1 \\ &\quad + [L_{g_2} h_2(x) + L_{\Delta g_2} h_2(x)] u_2 \end{aligned} \quad (24)$$

For the PV system, the state equations are derived as

$$\begin{aligned} \dot{\hat{z}}_1 &= -1.36\omega I_{1d} - 1.042 \frac{R}{L_1} I_q - 1.23 \frac{V_{cfd}}{L_1} + 1.18 \frac{V_{pv}}{L_1} K_q \\ \dot{\hat{z}}_2 &= \frac{1.16}{C} i_{pv} - \frac{1.08}{C} I_{1d} K_d - \frac{1.14}{C} I_{1q} K_q \end{aligned} \quad (25)$$

If \tilde{v}_1 and \tilde{v}_2 are considered as the linear control inputs, then the feedback-linearized PV system with uncertainties (25) can be represented by the following linear systems:

$$\begin{aligned} \dot{\hat{z}}_1 &= \tilde{v}_1 \\ \dot{\hat{z}}_2 &= \tilde{v}_2 \end{aligned} \quad (26)$$

Where

$$\begin{aligned} \tilde{v}_1 &= -1.36\omega I_{1d} - 1.042 \frac{R}{L_1} I_q - 1.23 \frac{V_{cfd}}{L_1} + 1.18 \frac{V_{pv}}{L_1} K_q \\ \tilde{v}_2 &= \frac{1.16}{C} i_{pv} - \frac{1.08}{C} I_{1d} K_d - \frac{1.14}{C} I_{1q} K_q \end{aligned} \quad (27)$$

The linear control laws and for the feedback linearized system (26) can be obtained using any standard linear control theory. The physical control inputs and of the PV system can be calculated from (27). But before obtaining these physical control laws, it is essential to analyze the stability of internal dynamics which is shown in the following step.

Step 2: Stability of internal dynamics.

In the previous step, the seventh-order PV system (9) is transformed into a second-order linear part (26), representing the linear dynamics of the system. For the transformed system, the desired performance can be obtained through the implementation of a partial feedback linearizing controller. But before implementing such controllers, it is essential to analyze the dynamics of the nonlinear part represented by the state \hat{z} , (15) and the dynamics of which are called internal dynamics. To ensure stability of any

feedback-linearized system, the control law needs to be chosen in such a way that

$$\lim_{t \rightarrow \infty} h_i(x) \rightarrow 0$$

which implies that the state of the linear system decays to zero as time approaches infinity, that is $[\tilde{z}_1 \ \tilde{z}_2 \ \dots \ \tilde{z}_r]^T \rightarrow 0; t \rightarrow \infty$. For the PV system considered in this paper, this means that at steady state

$$\begin{aligned} \tilde{z}_1 &= 0 \\ \tilde{z}_2 &= 0 \end{aligned} \quad (28)$$

Let us now consider the nonlinear state expressed by the function $\hat{z} = \widehat{\phi}(x)$ see (15). To ensure the stability of PV systems, this \hat{z} needs to be selected to satisfy the following conditions

$$\begin{aligned} L_{g1} \widehat{\phi}(x) &= 0 \\ L_{g2} \widehat{\phi}(x) &= 0 \end{aligned} \quad (29)$$

For the PV system, (29) is satisfied if we choose

$$\widehat{\phi}(x) = \hat{z} = \begin{bmatrix} \hat{z}_3 \\ \hat{z}_4 \\ \hat{z}_5 \\ \hat{z}_6 \\ \hat{z}_7 \end{bmatrix} = \begin{bmatrix} \frac{1}{2} LI_{1d}^2 + \frac{1}{2} LI_{1q}^2 + \frac{1}{2} C v_{pv}^2 \\ v_{cfd} \\ v_{cfq} \\ I_{2d} \\ I_{2q} \end{bmatrix} \quad (30)$$

Thus, the dynamics of $\hat{z} = \widehat{\phi}(x)$ can be expressed as

$$\dot{\hat{z}} = L_f \widehat{\phi}(x) \quad (31)$$

For \hat{z}_3 , the dynamics can be simplified as

$$\dot{\hat{z}}_3 = -\frac{2R}{L} \hat{z}_3 \quad (32)$$

which represents a stable system, and the dynamics of the remaining states can be calculated by using (31) as

$$\dot{\hat{z}}_i = 0 \quad \text{with } i=4,5,6 \text{ and } 7 \quad (33)$$

which represents marginal stability of the internal dynamics. Therefore, the robust partial feedback linearized controller can be designed and implemented for a three-phase grid-connected PV system with an output LCL filter. The derivation of the proposed robust control law is shown in the next step.

Step 3: Derivation of the robust control law.

From (27), the control law can be obtained as follows:

$$\begin{aligned} K_d &= \frac{0.85L}{v_{pv}} (\widetilde{v}_1 + 1.36\omega I_{1d} + \frac{1.042R}{L_1} I_{1q} + \frac{1.23v_{cfd}}{L_1}) \\ K_q &= -0.88 \frac{C}{I_q} \left[\widetilde{v}_2 + 1.16 \frac{i_{pv}}{C} - 1.08 \frac{I_{1d}}{C} K_d \right] \end{aligned} \quad (34)$$

Equation (34) is the final robust control law for a three-phase grid-connected PV system and the control law contains the model uncertainties. The main difference between the designed robust control law (34) and the control law is the inclusion of uncertainties within the PV system model. Here, the linear control inputs \widetilde{v}_1 and \widetilde{v}_2 and can be obtained in a similar way as discussed in before. The performance of the designed robust stabilization scheme is evaluated and compared in the following section to that without any uncertainty along with the direction of practical implementation.

VI. CONTROLLER PERFORMANCE EVALUATION

To evaluate the performance of the three-phase grid-connected PV with Wind system with the designed robust controller, a PV with Wind array with 20 strings each characterized by a rated current of 2.8735 A is used. Each string is subdivided into 20 modules characterized by a rated voltage of 43.5 V and connected in series. The total output voltage of the PV array is 870 V, the output current is 57.47 A, and the total output power is 50 kW. The value of the dc-link capacitor is 400 F, the line resistance is 0.1 Ω, and inductance is 10 mH. The grid voltage is 660 V and the frequency is 50 Hz. The switching frequency of the inverter is considered as 10 kHz.

The inclusion of LCL filter dynamics affects the stability of the system for which a peak amplitude response at the resonance frequency of the LCL filter exists, and if the parameters of

Then, the control law is obtained in the frame and, finally, reverse transformation (i.e., $(dq - abc)$) is done to implement the controller through the PWM.

MATLAB/SIMULINK OUTPUTS

Simulation diagram

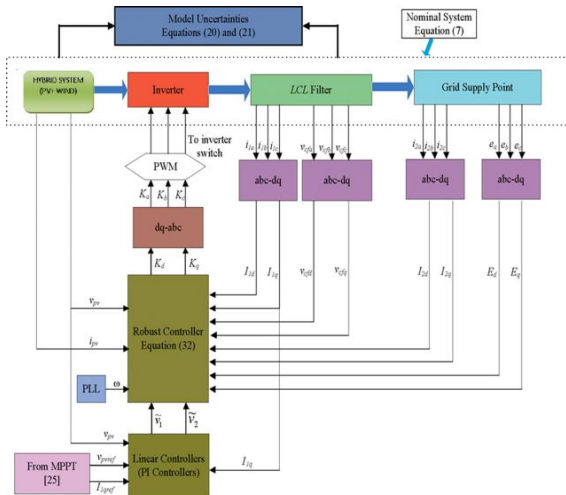
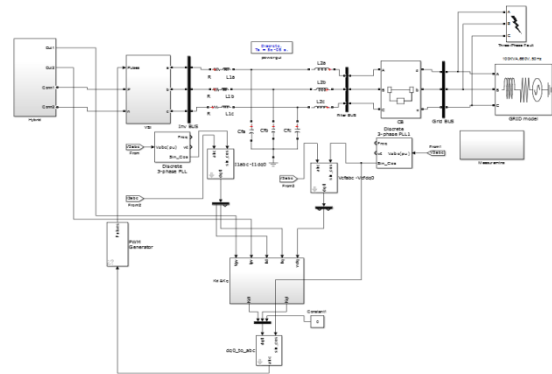
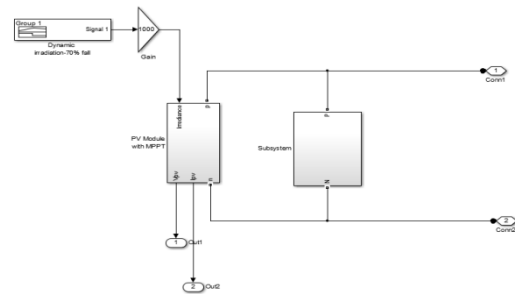


Fig. 3. Implementation block diagram.



PV and Wind power generation circuits

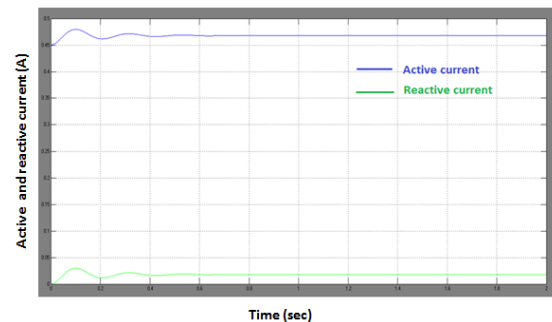


LCL filters are not chosen appropriately, the dynamic stability of the system will be degraded. To perform the simulation, the inductor and capacitor values of the LCL filter are selected based on the filter design process as presented in which are 10 mH and 3.1 μ F. Since partial feedback linearizing controllers are sensitive to system parameters, it is essential to have an exact system model in order to achieve good performance. But for real life grid connected PV with Wind systems, there often exist inevitable uncertainties in constructed models.

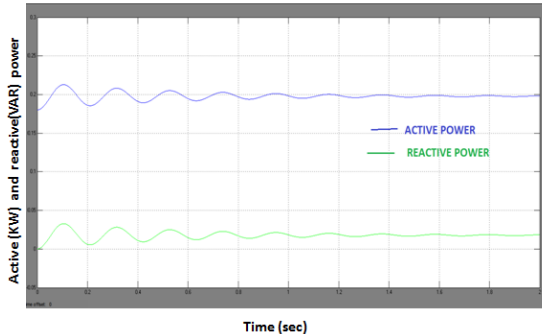
It is the type of hybrid energy system consists of photovoltaic array coupled with wind turbine. This would create more output from the wind turbine during the winter, whereas during the summer, the solar panels would produce their peak output.

In addition, uncertain parameters exist that are not exactly known or difficult to estimate. Therefore, to evaluate the performance of the designed robust control scheme, it is essential to consider these uncertainties. The implementation block diagram of the designed robust control scheme is shown in Fig. 3 where the nominal model of the PV with Wind system is shown along with the uncertainties. From Fig. 3, it can also be seen that the output currents of the three phase inverter, voltages across the filter capacitor, output currents of the filter, and grid voltages are transformed into direct— and quadrature-axis components using $abc - dq$ transformation.

Positive-sequence active and reactive current during the single-line-to-ground fault



Negative-sequence active and reactive power during the single-line-to-ground fault



CONCLUSIONS:

A robust controller is designed by modelling the uncertainties of a three-phase grid-connected PV system in a structured way based on the satisfaction of matching conditions to ensure the operation of the system at unity power factor. The partial feedback linearizing scheme is employed to obtain the robust control law and with the designed control scheme, only the upper bounds of the PV systems' parameters and states need to be known rather than network parameters, system operating points, or natures of the faults. The resulting robust controller enhances the overall stability of a three-phase grid-connected PV system considering admissible network uncertainties. Thus, this controller has good robustness against the changes in parameters and variations in atmospheric conditions irrespective of the network parameters and configuration. With the hybrid system and robust controller we can get improved outputs as compared with the normal system.

REFERENCES:

[1] I. Kim, "Sliding mode controller for the single-phase grid-connected photovoltaic system," *Appl. Energy*, vol. 83, pp. 1101–1115, 2006.

[2] I.-S. Kim, "Robust maximum power point tracker using sliding mode controller for the three-phase grid-connected photovoltaic system," *Solar Energy*, vol. 81, no. 3, pp. 405–414, Mar. 2007.

[3] A. O. Zue and A. Chandra, "State feedback linearization control of a grid connected photovoltaic interface with MPPT," presented at the IEEE Elect.

Power Energy Conf., Montreal, QC, Canada, Oct. 2009.

[4] D. Lalili, A. Mellit, N. Lourci, B. Medjahed, and E.M. Berkouk, "Input output feedback linearization control and variable step size MPPT algorithm of a grid-connected photovoltaic inverter," *Renew. Energy*, vol. 36, no. 12, pp. 3282–3291, Dec. 2011.

[5] M. A. Mahmud, H. R. Pota, and M. J. Hossain, "Dynamic stability of three-phase grid-connected photovoltaic system using zero dynamic design approach," *IEEE J. Photovolt.*, vol. 2, no. 4, pp. 564–571, Oct. 2012.

[6] V. Kaura and V. Blasko, "Operation of a phase locked loop system under distorted utility conditions," *IEEE Trans. Ind. Appl.*, vol. 33, no. 1, pp. 58–63, Jan. 1997.

[7] A. Isidori, *Nonlinear Control Systems..* Berlin, Germany: Springer-Verlag, 1989.

S. Behtash, "Robust output tracking for nonlinear systems," *Int. J. Control*, vol. 51, no. 6, pp. 1381–1407, 1990.

[9] M. A. Mahmud, M. J. Hossain, and H. R. Pota, "Selection of output function in nonlinear feedback linearizing excitation control for power systems," in *Proc. Australian Control Conf.*, 2011, pp. 458–463.

[10] M. A. Mahmud, H. R. Pota, and M. J. Hossain, "Zero dynamic excitation controller for multimachine power systems to augment transient stability and voltage regulation," in *Proc. IEEE Power Energy Soc. Gen. Meeting*, 2012, pp. 1–7.

[11] M. Liserre, F. Blaabjerg, and S. Hansen, "Design and control of an LCL-filter-based three-phase active rectifier," *IEEE Trans. Ind. Appl.*, vol. 41, no. 5, pp. 1281–1291, Sep. 2005.

[12] S.-K. Kim, J.-H. Jeon, C.-H. Cho, E.-S. Kim, and J.-B. Ahn, "Modeling and simulation of a grid-connected PV generation system for electromagnetic transient analysis," *Solar Energy*, vol. 83, no. 5, pp. 664–678, 2009.

[13] H. Karimi, A. Yazdani, and R. Iravani, "Negative-sequence current injection for fast islanding detection of a distributed resource unit," *IEEE Trans. Power Electron.*, vol. 23, no. 1, pp. 298–307, Jan. 2008.